Department of Respiratory Medicine[1]; Department of First Stationed Outpatient[2], the 940th Hospital of Joint Logistics Support Force of Chinese People's Liberation Amy; Forensic Identification Centre[3], Gansu University of Political Science and Law, Lanzhou, Gansu Province, China

Astragaloside IV attenuates TGF-β-mediated epithelial-mesenchymal transition of pulmonary fibrosis via suppressing NLRP3 expression *in vitro*

Yan Hou[1], Yingli Zhen[2], Qingliang Xue[1], Wei Wang[3,*]

Received November 23, 2020, accepted December 18, 2020

**Corresponding author: Wei Wang, Forensic Identification Centre, Gansu University of Political Science and Law, No. 6, West Anning Road, Gansu University of Political Science and Law, Lanzhou 730070, Gansu Province, China, E-mail: ww6761@hotmail.com*

Pharmazie 76: 97-102 (2021) *doi: 10.1691/ph.2021.0933*

Pulmonary fibrosis (PF) is a severe chronic disease. Although astragaloside IV (ASV) is known to have therapeutic effects on PF, the therapeutic targets of ASV require further study. This study was designed to elucidate the regulatory effect of ASV on PF via NLRP3. PF was triggered by transforming growth factor-β (TGF-β) *in vitro*. The relative activity of TGF-β was measured by luciferase reporter assay. Protein levels were determined by western blotting assay. The NLRP3 expression was analyzed using immunofluorescence analysis. mRNA levels were detected by qRT-PCR. MTT assay was performed to determine cell viability. Wound healing and transwell assays were conducted to investigate cell migration and invasion. We found that ASV markedly suppressed TGF-β activity, Smad2/3 and NLRP3 protein expression levels. ASV inhibited cell viability, migration and invasion ability. Moreover, ASV mediated downregulation of N-cadherin and Snail and upregulation of E-cadherin, which further suppressed the epithelial-mesenchymal transition (EMT). However, overexpression of NLRP3 reversed the effects of ASV and promoted Collagen I, Collagen II and α-SMA protein expressions. In conclusion, ASV efficiently retarded PF progress via suppressing NLRP3 expression *in vitro*.

1. Introduction

Pulmonary fibrosis (PF) is an irreversible, chronic, and often fatal lung disease caused by various risk factors (infection, environment, autoimmune disorders, drugs, genetic abnormalities) (Raghu et al. 2011). PF was typically characterized by subpleural lung tissue fibrosis, subepithelial fibroblast lesions, and microscopic honeycomb morphology changes. Studies revealed that the pathogenesis of PF involves multiple aspects, such as inflammation, excessive deposition of extracellular matrix (ECM) protein, and epithelial-mesenchymal transition (EMT) of pulmonary fibroblasts (Selman and Pardo 2002). Because of PF's insidious onset, there were often no obvious symptoms in the early stage. Furthermore, due to the unfavorable prognosis of PF, the patients usually die from respiratory failure or other complications with a median survival time of 2.5 to 3.5 years (Thickett et al. 2014). Pirfenidone and sildenafil were confirmed to have a relieving effect on the development of PF, while the therapeutic effect was limited (Behr et al. 2018; Sakamoto et al. 2013). Therefore, further exploring the pathogenesis of PF and seeking for potential targets may provide novel treatments for PF.

Epithelial-mesenchymal transition (EMT) is a critical pathological process of PF (Hill et al. 2019). Several studies found that about one-third of the fibroblasts originated from EMT (Han et al. 2018; Chen et al. 2014). During EMT progress, E-cadherin decreased, while smooth muscle actin (α-SMA), N-cadherin and Snail showed an inverse trend (Zhao et al. 2014). Transforming growth factor-β (TGF-β) exhibited a regulatory effect on fibrogenesis; it mediated PF occurrence *via* inducing EMT, inhibiting the apoptosis of lung epithelial cells, and synthesizing ECM proteins (Dinesh Babu et al. 2020).

Moreover, PF is generally accompanied by inflammation (He et al. 2010). NOD-like receptor family, pyrin domain-containing 3 (NLRP3) inflammasome is a multi-protein complex composed of NLRP1, ASC oligomer and cysteinyl aspartate specific proteinase-1 (caspase-1) (Zheng et al. 2018). Inflammation might aggravate the PF progress (Li et al. 2018), so alleviating the inflammatory response is also crucial for the PF treatment.

Astragaloside IV (ASV) is one of the main active ingredient in the traditional Chinese medicine *Astragalus* (Ren et al. 2013). Pharmacological studies on ASV suggested that it possesses anti-inflammation (Xu et al. 2016), anti-diabetes (Luo et al. 2016), and anti-hypertension properties (Luo et al. 2019). ASV reduced the hydroxyproline level in lung tissues and suppressed the TGF-β1 and TNF-α expressions to observably attenuate bleomycin-induced PF *in vivo* (Cui et al. 2015). Besides, ASV markedly downregulated the high mobility group protein 1 (HMGB1) level in serum and lung tissues and inhibited the pulmonary α-SMA expression. Li et al. (2017) indicated that ASV attenuated bleomycin-induced ECM deposition. Thence ASV may be a promising candidate for PF. However, whether ASV targets NLRP3 in PF or not remains unclear. This study aimed to explore the ASV regulation on EMT and inflammation, further to investigate the underlying regulatory mechanism of ASV on PF.

2. Investigations and results

2.1. ASV suppresses the activation of TGF-β pathways

The relative activity of TGF-β was lifted as the TGF-β reporter concentration increasing, which suggested a successful construction of the TGF-β luciferase reporter vector (Fig. 1A). However, ASV suppressed TGF-β relative activity (Fig. 1B) and mRNA expression level (Fig. 1C). In addition, the Smad2 and Smad3 expressions were elevated after TGF-β stimulation compared with the control group (Fig. 1D).

2.2. ASV inhibits the cell viability and EMT induced by TGF-β

MTT assay results suggested that TGF-β significantly promoted the cell viability, while ASV efficiently attenuated the viability of

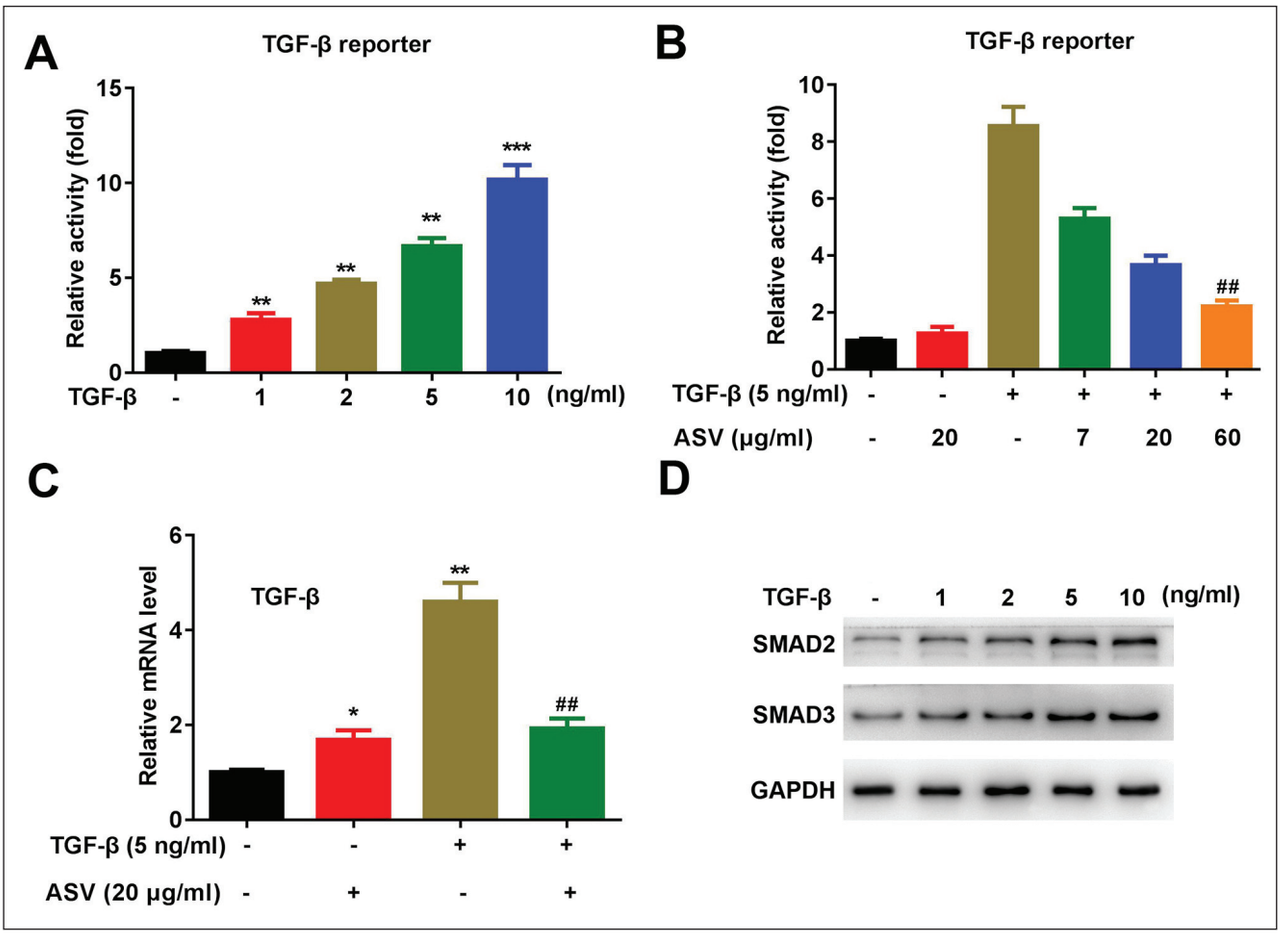

Fig. 1: Effects of ASV on the relative activity and mRNA level of TGF-β. (A) Relative activities of TGF-β in the cells treated with 0, 1, 2, 5, 10 ng/ml TGF-β. (B) Relative activities of TGF-β in the cells treated with 5 ng/ml TGF-β and/or 7, 20, 60 ng/ml ASV. (C) Relative mRNA expression levels of TGF-β in the cells treated with 5 ng/ml TGF-β and/or 20 ng/ml ASV. (D) Smad2 and Smad3 protein levels of the cells were analyzed by western blotting assay. *P<0.05 vs. TGF-β^{-}/ASV^{-}; **P<0.01 vs. TGF-β^{-} or TGF-β^{+}/ASV^{-}; ***P<0.001 vs. TGF-β^{-}; $^{\#\#}$P<0.01 vs. TGF-β^{+}/ASV^{-}. ASV, Astragaloside IV; TGF-β, transforming growth factor-β.

the TGF-β-treated cells (Fig. 2A). Wound healing and transwell experiments were conducted to investigate the effect of ASV on cell migration and invasion. As expected, the results exhibited a similar trend that the ASV treatment observably reduced the migration and invasion ability of the TGF-β-treated cells (Fig. 2B-2D). In addition, ASV treatment markedly suppressed N-cadherin and Snail expressions, and elevated E-cadherin expression (Fig. 2E).

2.3. ASV suppresses the expression of NLRP3

ASV significantly decreased the NLRP3 expression level of the TGF-β-treated cells (Fig. 3A and 3B). Moreover, the immunofluorescence staining showed that ASV markedly abated the increase of NLRP3 induced by TGF-β (Fig. 3C).

2.4. Overexpression of NLRP3 reverses the effects of ASV on fibrosis

The NLRP3 overexpression model was successfully established in the A549 cells (Fig. 4A). Western blotting results confirmed that ASV memorably prevented the fibrosis-related protein (Collagen I, Collagen II, α-SMA) expressions of TGF-β-induced cells, while NLRP3 enhanced the protein expressions inversely (Fig. 4B).

2.5. Overexpression of NLRP3 antagonizes the effects of cell viability and EMT cell

To further investigate the potential roles of NLRP3 in PF, cells were treated with NLRP3. Cell viability of the NLRP3 overexpression group was notably higher than that of the ASV-treated group after incubated for 48 h (Fig. 5A). As shown in Fig. 5B and 5C, overexpression of NLRP3 reversed the effects of ASV and induced migration and invasion of the TGF-β-treated cells. The effects of ASV on the expression of E-cadherin, N-cadherin and Snail were reversed by NLRP3 (Fig. 5D).

3. Discussion

The major findings of the present study demonstrated that ASV prevented cell viability, invasion and EMT progress in the TGF-β-induced cells, which may contribute to the relieve of PF. Furthermore, NLRP3 was confirmed to be downregulated following the ASV treatment, and overexpression of NLRP3 antagonized the inhibitory effects of ASV.

ASV is the main compound among the saponins identified from *Astragalus* root (Ren et al. 2013). In recent years, ASV has been reported to have protective effects on the cardiovascular (Hu et al. 2009), immune (Yuan et al. 2011), and hematopoietic systems (Li et al. 2011). Yu et al. (2016) found that ASV-mediated suppression of fibroproliferation might contribute to the anti-fibrotic effect against bleomycin (BLM)-induced PF. ASV notably reduced TGF-β1/PI3K/Akt-mediated Forkhead box O3 (FOXO3a) hyperphosphorylation and downregulation, and further prevented EMT during fibrogenesis (Qian et al. 2018). Long non-coding RNAs sirt1 antisense (lncRNA sirt1 AS) remarkably inhibited TGF-β1-mediated EMT *in vitro* and relieved PF *in vivo* (Qian et al. 2020). The present results exhibited that ASV treatment notably suppressed cell viability, migration, EMT and fibrosis progress of the TGF-β-induced cells, which were consistent with the previous studies.

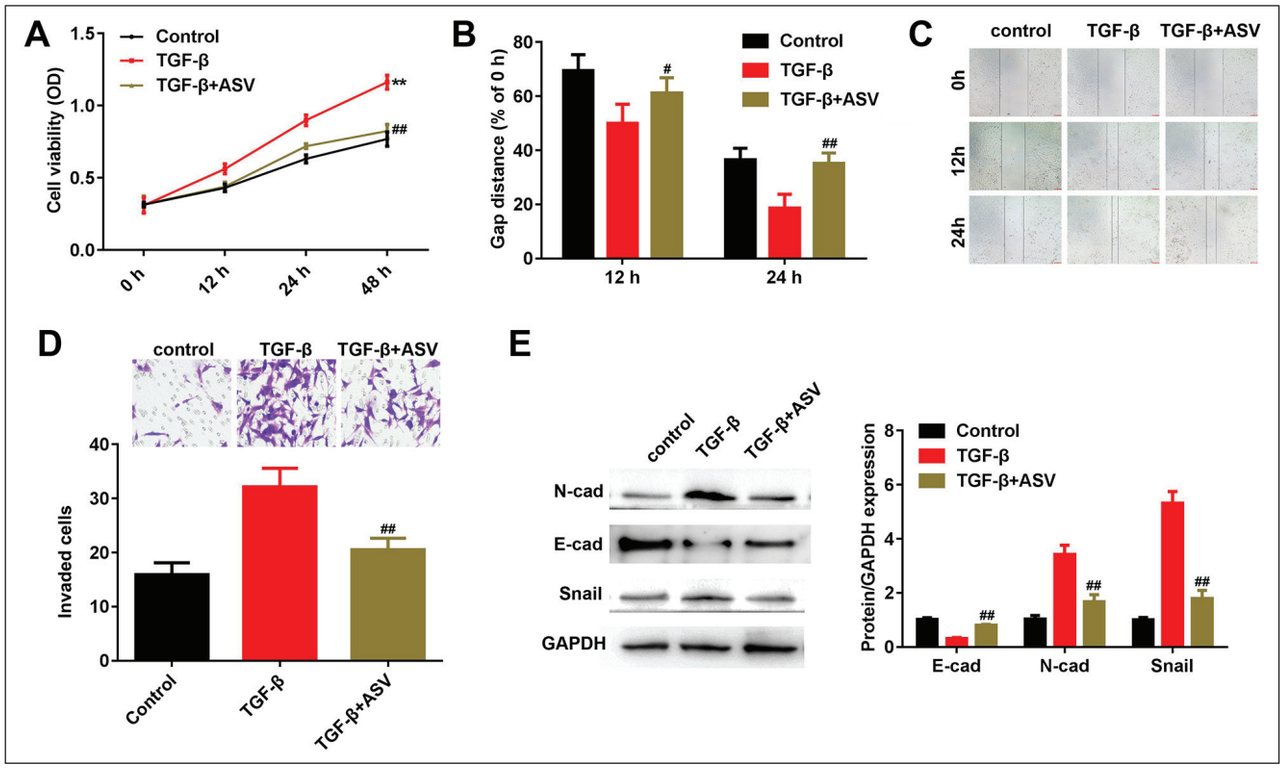

Fig. 2: ASV regulates the cell viability, migration and EMT progress. (A) Absorbance values of the cells treated with TGF-β or ASV/ TGF-β at 0, 12, 24, 48 h. (B) Wound healing and (C) transwell assays were conducted to determinate the cell migration of the cells treated with TGF-β or ASV/ TGF-β. (D) The numbers of migrated cells treated with TGF-β or ASV/ TGF-β. (E) Relative protein expression levels of E-cadherin, N-cadherin and Snail in the cells treated with TGF-β or ASV/ TGF-β compared with GAPDH. **P<0.01 vs. control; $^{\#}$P<0.05 vs. TGF-β; $^{\#\#}$P<0.01 vs. TGF-β. ASV, Astragaloside IV; TGF-β, transforming growth factor-β.

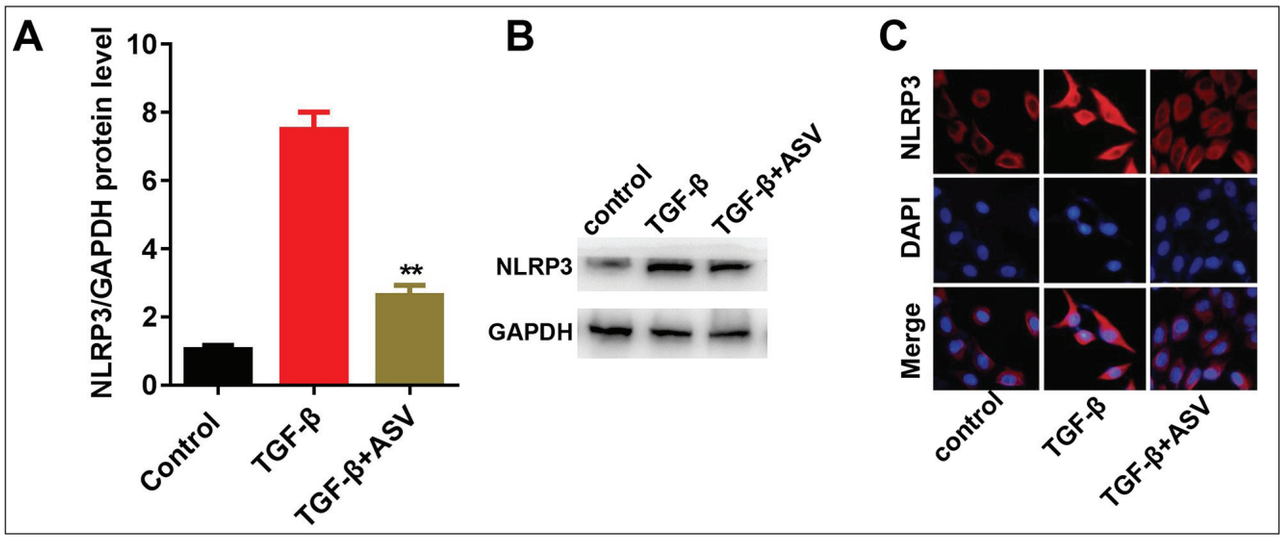

Fig. 3: Effect of ASV on NLRP3 protein expression of the cells treated with TGF-β or ASV/ TGF-β. (A and B) The protein expression levels of NLRP3 in the cells treated with TGF-β or ASV. (C) The expressions of NLRP3 in the cells treated with TGF-β or ASV/ TGF-β were analyzed using fluorescence microscopy analysis. **P<0.01 vs. TGF-β. ASV, Astragaloside IV; TGF-β, transforming growth factor-β; NLRP3, NLR Family Pyrin Domain Containing 3.

Epithelial cells exhibit apical-base polarity, they adhere and communicate with each other through specialized intercellular connections, and are located on the basement membrane (Thiery and Sleeman 2006). Under certain physiological or pathological conditions, epithelial cells could transform into mesenchymal cells, leading to a loss of cell polarity, decreased adhesion, and changes in the cytoskeleton, thereby promoting cell migration (Thiery et al. 2009). These physiological changes are called epithelial-mesenchymal transition (EMT). EMT is the basis of mammalian embryonic development. It is common in early embryonic development and is especially vital for organ formation and nervous system differentiation (Nieto 2009). Besides, EMT plays a pivotal role in inflammation, organ fibrosis and highly metastatic cancer (Pastushenko and Blanpain 2019). Previous studies reported that EMT is a crucial process during several types of organ fibrosis development, such as liver fibrosis (Kong et al. 2020), renal interstitial fibrosis (Wang et al. 2020) and pulmonary fibrosis (Willis et al. 2005). PF is characterized by aberrant extracellular matrix

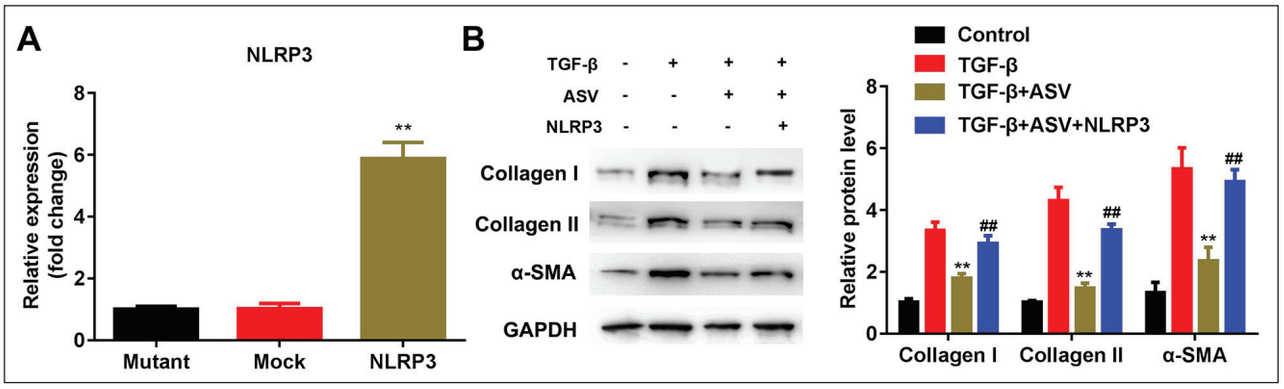

Fig. 4: Effect of NLRP3 overexpression on fibrosis-related proteins. (A) Relative expressions of NLRP3 in mutant, mock and NLRP3 group. (B) Relative protein expression levels of Collagen I, Collagen II and α-SMA in the cells treated with TGF-β, ASV or NLRP3. **P<0.01 vs. mutant or TGF-β; ##P<0.01 vs. TGF-β+ASV. ASV, Astragaloside IV; TGF-β, transforming growth factor-β; NLRP3, NLR Family Pyrin Domain Containing 3.

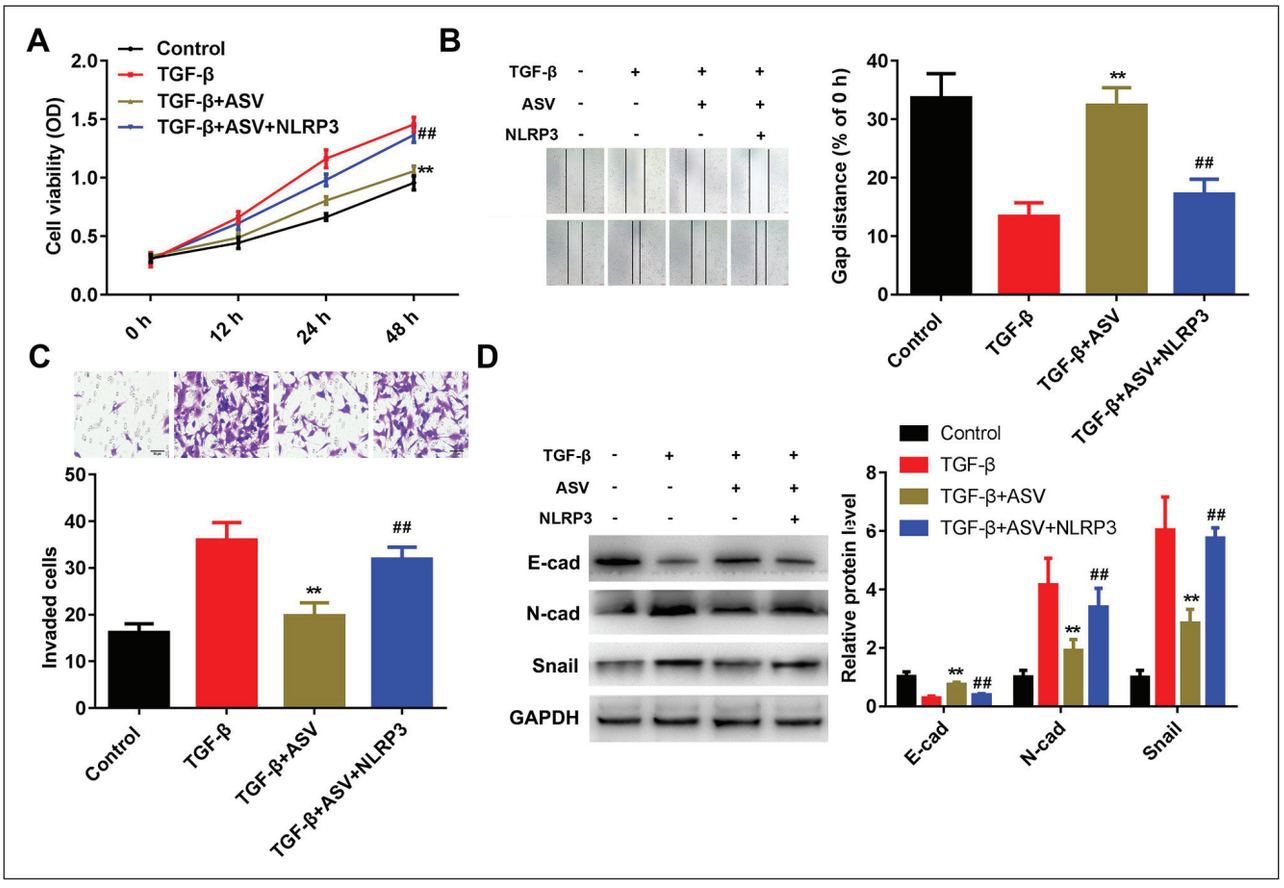

Fig. 5: Overexpression of NLRP3 reverses the effects of ASV. (A) Absorbance values of the cells treated with TGF-β, ASV or NLRP3 at 0, 12, 24, 48 h. (B) Wound healing and (C) transwell assays were conducted to determinate the cell migration of the cells treated with TGF-β, ASV or NLRP3. (D) Relative protein expression levels of E-cadherin, N-cadherin and Snail in the cells treated with TGF-β, ASV or NLRP3. **P<0.01 vs. TGF-β; ##P<0.01 vs. TGF-β+ASV. ASV, Astragaloside IV; TGF-β, transforming growth factor-β; NLRP3, NLR Family Pyrin Domain Containing 3.

(ECM) deposition by activated myofibroblasts, while EMT accelerated the production of ECM components, ulteriorly exacerbated cell migration and invasion (Guan et al. 2016). We treated the A549 cells with TGF-β and successfully mediated PF *in vitro*, as evidenced by a decreased protein expression level of E-cadherin and a enhancement in protein expression levels of N-cadherin and Snail.

NLRP3 is one of the structural subsets of the inflammasome (Artlett 2012), and inflammation is a major symptom of many lung injuries and diseases. For instance, many complications occurred after blood transfusion, of which transfusion-related acute lung injury induced by NLRP3 inflammasome was the leading cause (Land 2013). The reactive oxygen species (ROS) level was reported to be increased in the presence of chronic obstructive pulmonary disease (COPD), and the increment of ROS further activated the NLRP3 inflammasome (Muller et al. 2011). NLRP3 inflammasome that triggered by the inorganic particulates advanced IL-1β production. IL-1β was known to promote the expression level of TGF-β, ulteriorly aggravated PF (Liu 2008). The current study found that ASV efficiently suppressed NLRP3 expression in the TGF-β-me-

diated PF, while NLRP3 overexpression remarkably accelerated EMT development and fibrosis progress of the ASV-treated cells. The results suggested that ASV modulated NLRP3. However, the underlying mechanism of the ASV regulatory effect over NLRP3 requires further study.

In conclusion, these findings demonstrate that ASV could inhibit EMT and fibrosis progress *via* suppressing the NLRP3 protein expression *in vitro*, which suggests therapeutic effects of ASV and provides a new target for PF treatment.

4. Experimental

4.1. Culture condition and cell treatment

Human lung epithelial cell line (A549) was purchased from Procell. The cells were cultured in the regular DMEM with 10% FBS and 1% mycillin (all obtained from Gibco) at 37 °C in the presence of 5% CO_2. Trypsin (0.25%, Gibco) was added to the medium to adjust the cell concentration at $5x10^4$ cells/ml following the cell confluence reached 90%. To promote the EMT progress, the cells were then incubated with different concentration gradients of TGF-β after cell confluence reached 70%. ASV or/and NLRP3 were added to the cells under the research protocol. The treated cells were harvested for RNA and proteins isolation at the indicated time.

4.2. RNA extraction and quantitative real-time PCR (qRT-PCR)

The total cellular RNA was extracted by TRIzol (Invitrogen, Thermo Fisher Scientific, Inc.). cDNA was generated following the SuperScript™ IV (Invitrogen) kit's manual. qRT-PCR was conducted by SYBR Green Master Mix (Toyobo) on 7300 real-time PCR system (Applied Biosystems). The $2^{-\Delta\Delta Cq}$ method was used for calculating the fold changes of the corresponding gene and mRNA expression levels. The specific primers for the gene and mRNA were designed and synthesized by Shenggong Biotechnology Co., Ltd. The primer sequences were as follows: TGF-β (F: 5'-AGATTCAAGTCAACTGTGGAG-3', R: 5'-AAGCCCTGTATTC-CGTCTC-3'), NLRP3 (F: 5'-GTTTGACCCCGATGATGAGC-3', R: 5'-CTTGTG-GATGGGTGGGTTTG-3').

4.3. Luciferase reporter assay

The luciferase reporter vector of the wild-type TGF-β was constructed by Guangzhou RiboBio Co., Ltd. They were transfected into the A549 cells and incubated for 24 h. The cells were lysed to detect the luciferase activities using an illuminometer (Gossen).

4.4. MTT assay

The cells were resuspended and seeded into a 96-well plate at $1x10^4$ cells/well. Then the plate was cultured at 37 °C in the presence of 5% CO_2 and 100% humidity for 4 h after 50 µl MTT solution was added (Beyotime Institute of Biotechnology) to each well. Subsequently, the medium was discarded and 150 µl dimethyl sulfoxide (Macklin) solution was added to each well and mixed. The absorbance value was detected at 490 nm by a microplate reader (Mindray).

4.5. Wound healing assay

The cells were seeded into a 6-well plate. A line was perpendicularly scraped into the monolayer using a 10 µl micropipette tip after the cells were cultured at 37 °C in the presence of 5% CO_2 for 24 h. Next, the cells were washed three times with PBS (SolarBio) and cultured in a serum-free DMEM containing TGF-β, ASV or NLRP3 for 24 h. Images of the wounded area were observed and captured separately at 0, 12, and 24 h under an inverted microscope (SteREO Discovery, V20; Carl Zeiss AG).

4.6. Transwell assay

The cells in the logarithmic growth phase were collected and incubated in a serum-free DMEM for 24 h. Then the cells were resuspended at $1x10^5$ cells/ml. Each chamber was covered with 50 mg/L Matrigel matrix (BD Biosciences) before the cells were added to the apical chamber of a 24-well transwell chamber (8 µm pores; Corning). DMEM of the basolateral chamber contained 10% FBS, while the apical chamber did not. Subsequently, the cells were incubated at 37 °C with 5% CO_2 for 24 h. The apical chamber cells were wiped off using a wet cotton swab. Next, the basolateral chamber cells were fixed for 30 min using paraformaldehyde following stained for 20 min with 0.1% crystal violet. Finally, the transmembrane cells were photographed under an inverted microscope at a magnification of 200.

4.7. Western blotting assay

The A549 cells were washed three times with pre-chilled PBS after the medium was discarded. Then 200 µl RIPA buffer (Beyotime Institute of Biotechnology) was added to lyse the cells on ice for 30 min to extract the total protein. Protein concentration was determined by a BCA kit. Protein (20 µg) was separated by 12% SDS-PAGE at 120 v. The protein was transferred onto NC membranes (Sigma). After blocked with TBST containing 5% FBS for 2 h, the membranes were incubated with primary antibodies, such as anti-Collagen I (1:1000), anti-Collagen II (1:1000), anti-α-SMA (1:1000), anti-N-cadherin (1:1000), anti-E-cadherin (1:1000), anti-Snail (1:1000) and anti-GAPDH (1:3000, all from BioVision, Inc) at 4 °C in a shaking table overnight. GAPDH was used as an internal standard to normalize the protein levels. Finally, the horseradish peroxidase-conjugated secondary antibody (1:8000, BioVision, Inc) was incubated with the membranes under room temperature for 2 h. The bands were visualized with an ECL system (Thermo Scientific).

4.8. Immunofluorescence analysis

Paraformaldehyde (4%) in PBS was used to fix the cells, followed by blocking with 5% bovine serum albumin and 0.1% Triton X-100(both obtained from Beyotime Institute of Biotechnology). Subsequently, the cells were incubated with anti-NLRP3 primary antibody at 4 °C overnight. PBS was used to wash the cells three times prior to incubation with the second antibody. The cells were finally counterstained with DAPI (Beyotime Institute of Biotechnology). Images were obtained by fluorescence microscopy at a magnification of 200.

4.9. Statistical analysis

GraphPad Prism (version 8.2.1.441, GraphPad Software Inc.) was used to analyze the data. The results were expressed as mean±SD. Student t-test was performed for the comparison between 2 groups, whereas the analysis of variance (ANOVA) was used for the comparison among multiple groups. Pearson's coefficient was used for correlation analysis. $P<0.05$ was considered to indicate a statistically significant difference.

Acknowledgments: This study was financially supported by Forensic Identification Centre Research Funding project of Gansu Univerity of Political Science and Law (Grant No. jdzxyb2018-04) and Gansu Province Science and Technology Planning Project (Grant No. 20CX9ZA086).

Conflict of Interest: None declared.

References

Artlett CM (2012) The role of the NLRP3 inflammasome in fibrosis. Open Rheumatol J 6: 80–86.

Behr J, Nathan SD, Harari S, Wuyts W, Kirchgaessler KU, Bengus M, Gilberg F, Wells AU (2018) Sildenafil added to pirfenidone in patients with advanced idiopathic pulmonary fibrosis and risk of pulmonary hypertension: A Phase IIb, randomised, double-blind, placebo-controlled study – Rationale and study design. Respir Med 138: 13–20.

Chen T, Nie H, Gao X, Yang J, Pu J, Chen Z, Cui X, Wang Y, Wang H, Jia G (2014) Epithelial-mesenchymal transition involved in pulmonary fibrosis induced by multi-walled carbon nanotubes via TGF-beta/Smad signaling pathway. Toxicol Lett 226: 150–162.

Cui W, Li L, Li D, Mo X, Zhou W, Zhang Z, Xu L, Zhao P, Qi L, Li P, Gao J (2015) Total glycosides of Yupingfeng protects against bleomycin-induced pulmonary fibrosis in rats associated with reduced high mobility group box 1 activation and epithelial-mesenchymal transition. Inflamm Res 64: 953–961.

Dinesh Babu V, Suresh Kumar A, Sudhandiran G (2020) Diosgenin inhibits TGF-beta1/Smad signaling and regulates epithelial mesenchymal transition in experimental pulmonary fibrosis. Drug Chem Toxicol 2020: 1–12.

Guan R, Wang X, Zhao X, Song N, Zhu J, Wang J, Wang J, Xia C, Chen Y, Zhu D, Shen L (2016) Emodin ameliorates bleomycin-induced pulmonary fibrosis in rats by suppressing epithelial-mesenchymal transition and fibroblast activation. Sci Rep 6: 35696.

Han Q, Lin L, Zhao B, Wang N, Liu X (2018) Inhibition of mTOR ameliorates bleomycin-induced pulmonary fibrosis by regulating epithelial-mesenchymal transition. Biochem Biophys Res Commun 500: 839–845.

He X, Mekasha S, Mavrogiorgos N, Fitzgerald KA, Lien E, Ingalls RR (2010) Inflammation and fibrosis during Chlamydia pneumoniae infection is regulated by IL-1 and the NLRP3/ASC inflammasome. J Immunol 184: 5743–5754.

Hill C, Jones MG, Davies DE, Wang Y (2019) Epithelial-mesenchymal transition contributes to pulmonary fibrosis via aberrant epithelial/fibroblastic cross-talk. J Lung Health Dis 3: 31–35.

Hu JY, Han J, Chu ZG, Song HP, Zhang DX, Zhang Q, Huang YS (2009) Astragaloside IV attenuates hypoxia-induced cardiomyocyte damage in rats by upregulating superoxide dismutase-1 levels. Clin Exp Pharmacol Physiol 36) :351–357.

Kong D, Zhang Z, Chen L, Huang W, Zhang F, Wang L, Wang Y, Cao P, Zheng S (2020) Curcumin blunts epithelial-mesenchymal transition of hepatocytes to alleviate hepatic fibrosis through regulating oxidative stress and autophagy. Redox Biol 36: 101600.

Land WG (2013) Transfusion-related acute lung injury: the work of DAMPs. Transfus Med Hemother 40: 3–13.

Li LC, Xu L, Hu Y, Cui WJ, Cui WH, Zhou WC, Kan LD (2017) Astragaloside IV improves bleomycin-induced pulmonary fibrosis in rats by attenuating extracellular matrix deposition. Front Pharmacol 8: 513.

Li X, Yan X, Wang Y, Wang J, Zhou F, Wang H, Xie W, Kong H (2018) NLRP3 inflammasome inhibition attenuates silica-induced epithelial to mesenchymal transition (EMT) in human bronchial epithelial cells. Exp Cell Res 362: 489–497.

Li YR, Cao W, Guo J, Miao S, Ding GR, Li KC, Wang J, Guo GZ (2011) Comparative investigations on the protective effects of rhodioside, ciwujianoside-B and astragaloside IV on radiation injuries of the hematopoietic system in mice. Phytother Res 25: 644–653.

Liu RM (2008) Oxidative stress, plasminogen activator inhibitor 1, and lung fibrosis. Antioxid Redox Signal 10: 303–319.

Luo X, Huang P, Yuan B, Liu T, Lan F, Lu X, Dai L, Liu Y, Yin H (2016) Astragaloside IV enhances diabetic wound healing involving upregulation of alternatively activated macrophages. Int Immunopharmacol 35: 22–28.

Luo Y, Wan Q, Xu M, Zhou Q, Chen X, Yin D, He H, He M (2019) Nutritional preconditioning induced by astragaloside on isolated hearts and cardiomyocytes against myocardial ischemia injury via improving Bcl-2-mediated mitochondrial function. Chem Biol Interact 309: 108723.

Muller T, Vieira RP, Grimm M, Durk T, Cicko S, Zeiser R, Jakob T, Martin SF, Blumenthal B, Sorichter S, Ferrari D, Di Virgillio F, Idzko M (2011) A potential role for P2X7R in allergic airway inflammation in mice and humans. Am J Respir Cell Mol Biol 44: 456–464.

Nieto MA (2009) Epithelial-mesenchymal transitions in development and disease: old views and new perspectives. Int J Dev Biol 53: 1541–1547.

Pastushenko I, Blanpain C (2019) EMT Transition states during tumor progression and metastasis. Trends Cell Biol 29: 212–226.

Qian W, Cai X, Qian Q (2020) Sirt1 antisense long non-coding RNA attenuates pulmonary fibrosis through sirt1-mediated epithelial-mesenchymal transition. Aging 12: 4322–4336.

Qian W, Cai X, Qian Q, Zhang W, Wang D (2018) Astragaloside IV modulates TGF-beta1-dependent epithelial-mesenchymal transition in bleomycin-induced pulmonary fibrosis. J Cell Mol Med 22: 4354–4365.

Raghu G, Collard HR, Egan JJ, Martinez FJ, Behr J, Brown KK, Colby TV, Cordier JF, Flaherty KR, Lasky JA, Lynch DA, Ryu JH, Swigris JJ, Wells AU, Ancochea J, Bouros D, Carvalho C, Costabel U, Ebina M, Hansell DM, Johkoh T, Kim DS, King TE, Jr., Kondoh Y, Myers J, Muller NL, Nicholson AG, Richeldi L, Selman M, Dudden RF, Griss BS, Protzko SL, Schunemann HJ, Fibrosis AEJACoIP (2011) An official ATS/ERS/JRS/ALAT statement: idiopathic pulmonary fibrosis: evidence-based guidelines for diagnosis and management. Am J Respir Crit Care Med 183: 788–824.

Ren S, Zhang H, Mu Y, Sun M, Liu P (2013) Pharmacological effects of Astragaloside IV: a literature review. J Tradit Chin Med 33: 413–416.

Sakamoto S, Itoh T, Muramatsu Y, Satoh K, Ishida F, Sugino K, Isobe K, Homma S (2013) Efficacy of pirfenidone in patients with advanced-stage idiopathic pulmonary fibrosis. Intern Med 52: 2495–2501.

Selman M, Pardo A (2002) Idiopathic pulmonary fibrosis: an epithelial/fibroblastic cross-talk disorder. Respir Res 3: 3.

Thickett DR, Kendall C, Spencer LG, Screaton N, Wallace WA, Pinnock H, Bott J, Pigram L, Watson S, Millar AB (2014) Improving care for patients with idiopathic pulmonary fibrosis (IPF) in the UK: a round table discussion. Thorax 69: 1136–1140.

Thiery JP, Acloque H, Huang RY, Nieto MA (2009) Epithelial-mesenchymal transitions in development and disease. Cell 139: 871–890.

Thiery JP, Sleeman JP (2006) Complex networks orchestrate epithelial-mesenchymal transitions. Nat Rev Mol Cell Biol 7: 131–142.

Wang Y, Zhou Q, Tang R, Huang Y, He T (2020) FoxM1 inhibition ameliorates renal interstitial fibrosis by decreasing extracellular matrix and epithelial-mesenchymal transition. J Pharmacol Sci 143 : 281–289.

Willis BC, Liebler JM, Luby-Phelps K, Nicholson AG, Crandall ED, du Bois RM, Borok Z (2005) Induction of epithelial-mesenchymal transition in alveolar epithelial cells by transforming growth factor-beta1: potential role in idiopathic pulmonary fibrosis. Am J Pathol 166: 1321–1332.

Xu H, Wang CY, Zhang HN, Lv CY, Wang YZ (2016) Astragaloside IV suppresses inflammatory mediator production in synoviocytes and collageninduced arthritic rats. Mol Med Rep 13: 3289–3296.

Yu WN, Sun LF, Yang H (2016) Inhibitory effects of astragaloside IV on bleomycin-induced pulmonary fibrosis in rats via attenuation of oxidative stress and inflammation. Inflammation 39: 1835–1841.

Yuan X, Sun S, Wang S, Sun Y (2011) Effects of astragaloside IV on IFN-gamma level and prolonged airway dysfunction in a murine model of chronic asthma. Planta Med 77: 328–333.

Zhao H, Wu QQ, Cao LF, Qing HY, Zhang C, Chen YH, Wang H, Liu RY, Xu DX (2014) Melatonin inhibits endoplasmic reticulum stress and epithelial-mesenchymal transition during bleomycin-induced pulmonary fibrosis in mice. PLoS One 9: e97266.

Zheng R, Tao L, Jian H, Chang Y, Cheng Y, Feng Y, Zhang H (2018) NLRP3 inflammasome activation and lung fibrosis caused by airborne fine particulate matter. Ecotoxicol Environ Saf 163: 612–619.